Phagocytosis Independent Extracellular Nanoparticle Clearance by Human Immune Cells

ARTICLE *in* NANO LETTERS · DECEMBER 2009

Impact Factor: 13.59 · DOI: 10.1021/nl902830x · Source: PubMed

4 AUTHORS, INCLUDING:

Matthias Bartneck
RWTH Aachen University
38 PUBLICATIONS **542** CITATIONS
SEE PROFILE

Jürgen Groll
University of Wuerzburg
127 PUBLICATIONS **2,400** CITATIONS
SEE PROFILE

NANO LETTERS

pubs.acs.org/NanoLett

Phagocytosis Independent Extracellular Nanoparticle Clearance by Human Immune Cells

Matthias Bartneck,[†] Heidrun A. Keul,[§] Gabriele Zwadlo-Klarwasser,[*,†,‡] and Jürgen Groll[*,§]

[†]Interdisciplinary Centre for Clinical Research (IZKF) BioMAT, [‡]Department of Dermatology, University Hospital, Rhine-Westphalia Institute of Technology (RWTH), Aachen, Germany, and [§]DWI e.V. and Institute of Technical and Macromolecular Chemistry, RWTH Aachen University, Aachen, North Rhine-Westphalia, Germany

ABSTRACT It has recently been discovered that human immune cells, especially neutrophil granulocytes, form neutrophil extracellular traps (NETs) that abolish pathogens. Our study provides evidence that extracellular traps formed by neutrophils, monocytes and macrophages act as physical barriers for nanoparticles, thus presenting a new nanomaterial clearance mechanism of the human immune system. While particle shape is of minor importance, positive charges significantly enhance particle trapping.

KEYWORDS Gold nanorods, human immune cells, nanoparticle clearance

When bacteria or nanoparticles enter the human body, they are immediately confronted with the innate part of the human immune system. As integral components, monocytes and neutrophil granulocytes circulate in the bloodstream and readily eliminate pathogens or clear particles.[1,2] Human neutrophil granulocytes are ten times more numerous (4000− 7000 cells per μL of blood) than monocytes, but the latter can differentiate into longer-lived cell types such as dendritic cells or macrophages with various subtypes[3] that are present in various tissues. Bacteria phagocytized by neutrophils are killed with antimicrobial proteins, reactive oxygen species and proteolytic enzymes.[4] Five years ago it became evident that in addition to the phagocytic mechanisms, neutrophil granulocytes release structures into the extracellular space that mainly consist of DNA and protein and trap pathogens at infection sites (neutrophil extracellular traps (NETs)).[5] These structures contain a variety of antibacterial proteins from azurophilic granules. Recent reports have shown that the formation of extracellular traps is not restricted to neutrophils but they are formed as well by mast cells for entrapping pathogens.[6]

It is well-known that nanoparticles are rapidly internalized by immune cells when the particle surface is not adjusted to minimize interaction,[7] for example, by surface grafting of poly(ethylene oxide) (PEO). Very recently, we have studied the interaction of a gold-nanoparticle library with primary human immune cells and found that for nanoparticles, uptake mechanisms may rather be classified as macropinocytosis than phagocytosis.[8] Moreover, nanoparticle shape was found to strongly influence uptake by primary human immune cells, as nanorods are taken up significantly faster than nanospheres. However, up to now no studies have been performed to examine whether extracellular NETs may trap nanoparticles and thus act as additional clearance mechanism in the human body.

In this work, we exclusively use human primary immune cells to study the formation of NETs by neutrophils and other important immune cell populations. We examine the interaction of a model library of gold nanoparticles (AuNP) with spherical and rodlike shape and a variety of surface chemistries with these extracellular structures. AuNP bigger than 10 nm are generally considered biocompatible and show low cytotoxicity.[9] They can be produced with different shapes and their surface chemistry can readily be tailored. Furthermore, they are easy to detect either with TEM or by electroless-deposition. These properties predetermine them as model particles for interaction studies.

Gold nanorods (AuNR) were synthesized by Ag(I)-assisted seeded growth as reported before[10,11] (for a detailed description see Supporting Information section 1). TEM micrographs (Figure S1A, Supporting Information) show homogeneity of the samples with only very few spherical particle impurities. Exchange of cetyl-trimethylammonium-bromide (CTAB) with PEO was performed with different types of commercially available 3 kDa α,ω-bifunctional PEOs that bear a thiol group at the one and either an alcohol, amino-, or carboxy-group at the other end of the polymer chain. UV−vis spectroscopy (Figure S1B, Supporting Information) showed that the aspect ratio of the nanorods, characterized by the absorption band at 850 nm, was not affected by the coating procedure. For commercial gold nanospheres with 15 nm diameter (AuNS), citrate was

* To whom correspondence should be addressed. (J.G.) E-mail: groll@dwi.rwth-aachen.de. Phone: +492418023343. (G.Z.-K.) E-mail: gzwadlo-klarwasser@ukaachen.de. Phone: +492418088377.

Received for review: 08/30/2009
Published on Web: 12/08/2009

DOI: 10.1021/nl902830x | *Nano Lett.* **2010,** *10,* 59-63

exchanged with CTAB for comparability with AuNR. Coating of AuNPs with the polymeric compounds was done according to the same protocol for all nanoparticles and was characterized by means of ζ-potential measurements before and after polymer coating of the particles. Measurements were performed at pH 4 since the particle solutions after ligand exchange exhibit this pH and thus differences in ζ-potential were most significant under these conditions. Because of the positive charge of the CTA^+ ions, AuNR and AuNS stabilized by CTAB exhibit a strongly positive surface potential of +90 and about +50 mV, respectively. After ligand exchange and purification the solutions exhibit different ζ-potential values depending on the functional groups of the polymers and on the pH of the solution with a negative ζ-potential for carboxy-terminated PEO coatings (−20 mV) and a positive ζ-potential (+21 mV) for the amine-functional PEO. The surface modification with linear HS−PEO−OH leads to ζ-potentials in the range of 0 to −5 mV (Table S1, Supporting Information). In PBS buffered solution at physiological pH 7.4, the obtained absolute values are smaller, but the measurements show identical tendencies with positive ζ-potential of the CTAB and amine-terminated PEO-coated rods and a negative ζ-potential of the carboxy-functional PEO-coated rods (Table S2, Supporting Information). These results show that PEO-stabilized AuNP with hydroxyl-, amine- or carboxy-groups on the particle surface were obtained.

Granulocytes were isolated using dextrane sedimentation of whole blood followed by Ficoll density centrifugation. Peripheral blood mononuclear cells (PBMC) were isolated using Ficoll-Paque. Monocytes and lymphocytes were isolated from PBMC by subsequent magnetic bead separation or plastic adherence, respectively. To obtain monocyte-derived macrophages (MDM), monocytes were cultured for seven days in RPMI1640 medium with 5% autologous human serum. Immature and mature dendritic cells were obtained from monocytes using cytokines as described previously.[12,13] Transmission electron microscopy and electrolessless deposition were used to detect gold nanoparticles (for details see Supporting Information section 2).

This study concerns the interaction of nanoparticles with extracellular structures and networks secreted by human immune cells. Upon incubation of primary human leukocytes with AuNPs, we denoted that in addition to and independent of the uptake of gold nanoparticles, human immune cells release components into the extracellular space that result in the formation of networks consisting of cells, extracellular traps, and particles. Neutrophil granulocytes led to the highest percentage of cells involved in network formation (25.1%) that was significantly different from all other cell types ($p < 0.001$). Interestingly, also monocytes (3.9%) and macrophages (1.5%) produced such extracellular structures. Lymphocytes and dendritic cells did not produce networks (Figure 1). The fact that monocytes also form extracellular traps can be attributed to the common progenitor cell from which granulocytes and monocytes evolve.[14] Human monocytic cells are extremely diverse as they can be used for the generation of mast cells[15] and recently were used for the generation of stem cells.[16] This may explain their multiple interaction modes with

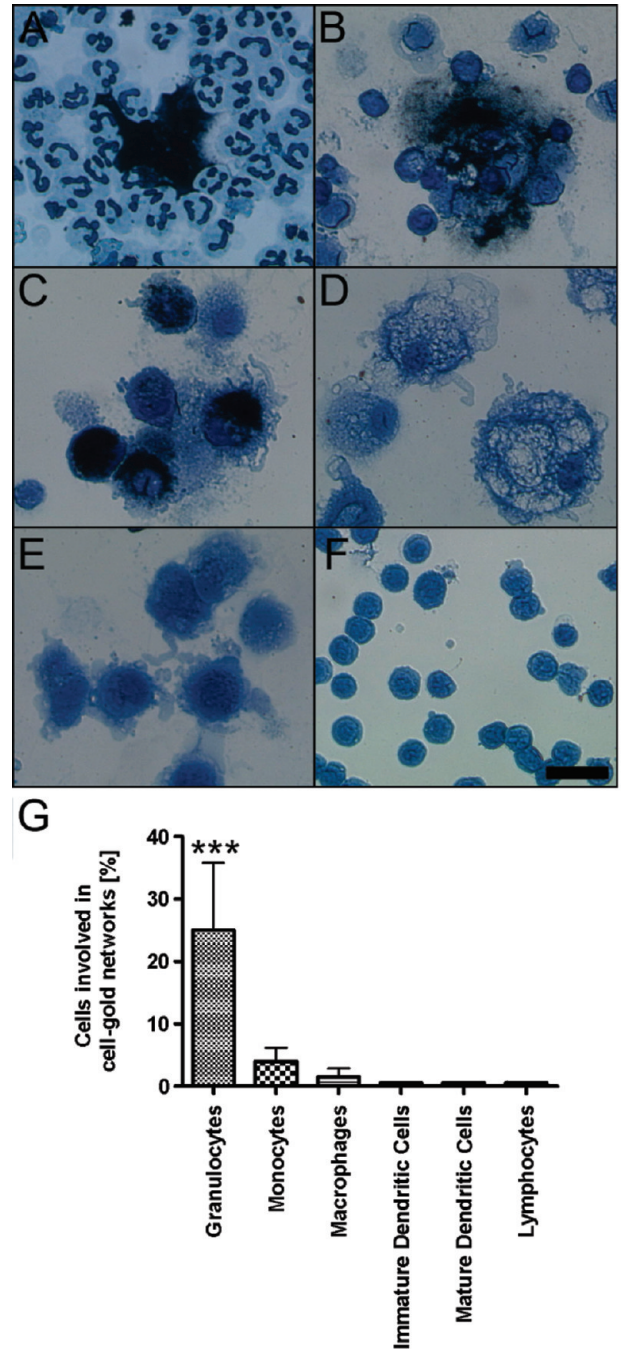

FIGURE 1. Different human immune cells located in cell-gold networks after 15 min of incubation with gold nanoparticles. (A) Neutrophil granulocytes formed the significantly highest amount of cell-gold networks ($P < 0.001$), less were induced by monocytes (B) and the fewest were found with macrophages (C). Immature (D) and mature dendritic cells (E) as well as lymphocytes (F) did not form such networks. (G) Percent of the various cell populations involved in NET formation. Bar (A−F) = 25 μm. Mean values ± standard deviation, $N = 6$.

DOI: 10.1021/nl902830x | *Nano Lett.* **2010,** *10,* 59-63

TABLE 1. Relative Portion of Granulocytes Involved in Network Formation after Incubation with Gold Nanorods (Middle) and Related Portion of Networks Containing Nanoparticles (Right) after 15 and 60 min of Incubation, Including Control Experiments with DNase and Cytochalasin D Treatment As Well As Cells without Nanoparticles (Mean Values ± Standard Deviation, $N = 6$)

		percent of cells involved in the networks		percent of networks containing AuNPs	
type of nanoparticle	surface modification and treatment	15 min	60 min	15 min	60 min
control without nanoparticles		25.4 ± 9.5	32.5 ± 8.6	0	0
AuNR15×50nm	HS−PEO−OH	18.9 ± 7.2	29.8 ± 11.2	15.1 ± 7.1	12.2 ± 5.1
	HS−PEO−COOH	22.6 ± 6.2	30.5 ± 11.5	13.2 ± 3.7	13.1 ± 6.2
	HS−PEO−NH_2	21.5 ± 8.3	32.6 ± 13.6	72.7 ± 12.0	76.2 ± 13.2
	CTAB	25.1 ± 12.8	34.8 ± 14.1	91.2 ± 9.8	88.2 ± 6.8
	CTAB + SFM[a]	35.4 ± 13.5	44.5 ± 17.2	94.0 ± 7.4	93.5 ± 8.0
	CTAB + DNase	4.2 ± 1.5	5.1 ± 1.2	92.6 ± 6.5	95.5 ± 5.5
	CTAB + Cyt D[b]	23.9 ± 11.4	35.8 ± 13.0	88.2 ± 7.5	82.6 ± 12.9
AuNS D=15nm	HS−PEO−OH	22.6 ± 10.5	27.6 ± 11.0	12.1 ± 3.5	12.2 ± 4.2
	CTAB	24.8 ± 8.5	36.9 ± 8.9	89.7 ± 9.8	91.2 ± 8.4
	CTAB + SFM[a]	32.9 ± 9.0	42.6 ± 12.2	93.4 ± 7.0	94.0 ± 7.4
	CTAB + DNase	3.5 ± 1.5	3.1 ± 0.8	91.2 ± 8.6	93.0 ± 8.8
	CTAB + Cyt D[b]	24.0 ± 5.0	22.5 ± 6.0	89.5 ± 9.1	88.0 ± 8.2

[a] SFM = serum free medium. [b] Cyt D = Cytochalasin D.

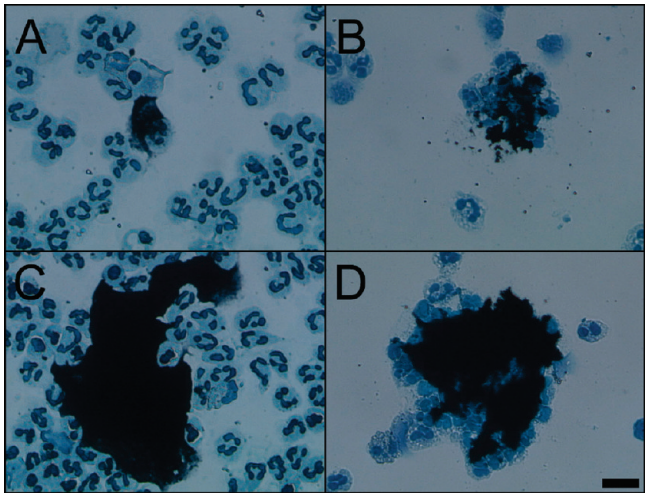

FIGURE 2. Cytospin preparations of granulocytes after incubation with CTAB- (A,C) and PEO-stabilized (B,D) gold nanorods (O.D. 0.5). Sizes of the cell-gold networks vary from two up to several dozens (C and D) of cells. Bar = 30 μm.

nanoparticles, comprising particle internalization[8] and trapping by extracellular structures, while neutrophil granulocytes mainly trap nanoparticles via the extracellular networks.

Cytospin preparations with differently modified nanoparticles were performed to elucidate the impact of particle surface chemistry and particle shape on the gold content inside the networks formed by neutrophil granulocytes (Table 1). Formation of the structures occurred rapidly within 15 min with about one-third further increase of involved cells after 60 min. The sizes of cell-gold formations vary from two (Figure 2 A and B) up to several dozens of cells (Figure 2 C and D). Nanorod surface chemistry had a negligible influence on network formation but a strong impact on the relative percentage of networks bearing gold. Positively charged particles (CTAB- as well as PEO−NH_2-coated) were more frequently (72− 92%) located inside the structures than PEO−OH or PEO−COOH-stabilized particles (12− 15%). Monocytes and macrophages generally showed a smaller portion of interconnected cells. The relative amount of trapped particles was not significantly different for 15 nm AuNS compared to AuNR at corresponding optical density and the same coatings (Table 1). This is in contrast to particle uptake, where particle shape does significantly influence the kinetics of particle internalization,[8] underlining the difference of the two particle clearance mechanisms. When the experiment was performed with nanoparticles at higher concentrations of O.D. > 1, aggregations of nanoparticles and cells became huge (several mm), stuck to the pipet tip and sometimes were solid like a tissue sample. This kind of aggregation may cause serious problems when occurring in vivo, so that such tests should be performed with nanoparticles that are intended for corresponding applications to identify the threshold concentration for this aggregate formation.

When the cells were incubated with the nanoparticles in serum free medium, the ratio of cells that are involved in network formation increased and the networks were formed more rapidly. The enhanced NET formation under serum free conditions indicates that serum proteins are involved in the regulation of NET formation which may in vivo regulate the spreading of the structures. A regulating effect of serum proteins is known for phagocytosis where inhibiting effects of certain serum proteins can be overcome by using serum free medium.[17]

After one day of culture on the glass slides, the NETs could still be detected. As expected, DNase treatment significantly decreased the percentage of cells involved in the formation of network structures whereas gold was still detectable, demonstrating the importance of DNA as constituent of the structures. Staining with 4′-6-diamidino-2-phenylindole (DAPI), a DNA-intercalating agent, resulted in blue colorization of the aggregates that additionally proved the presence of DNA in the structures (Figure 3A). When the structures

DOI: 10.1021/nl902830x | *Nano Lett.* **2010,** *10,* 59-63

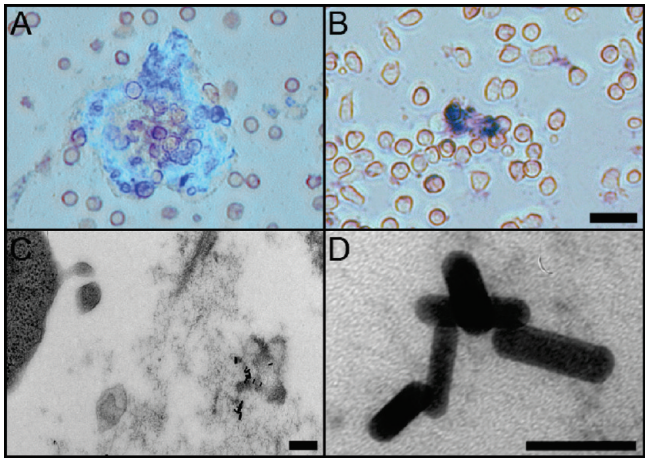

FIGURE 3. Neutrophil granulocytes after incubation with CTAB-coated gold nanorods. (A) DAPI staining of immobilized cells demonstrated that the structures in which gold nanorods were entrapped consisted of DNA (blue staining), the major constituent of neutrophil extracellular traps. (B) Structure formation could be abrogated using DNase. (C) Ultrathin sections revealed that the particles were located extracellular and (D) stuck inside extracellular traps and were not surrounded by a membrane. Bar (A,B) = 20 μm, (C) = 200 nm and (D) = 50 nm.

were treated with DNase prior to staining, no blue coloration was obtained (Figure 3B), demonstrating that DNA is a main constituent of the structures. This is in accordance to previous work in which NETs were visualized using the DNA-intercalating agent SytoxOrange.[7] However, gold was still detectable in the residual matrices that remain. We hypothesize that protein components from the NETs remain that are not affected by DNase treatment and thus may still trap nanoparticles. As the negatively charged DNA molecule is the major component of NET structures, electrostatic forces may be an explanation for the efficient trapping process of positively charged particles.

Treatment with Cytochalasin D, an inhibitor of actin polymerization and thus inhibitor of classical phagocytosis, had no inhibiting effects on network formation and on cell-gold matrix formation. This underlines independency of extracellular gold trapping from endocytosis. Inhibition of the structures by DNase demonstrates that the adhesiveness between cells and nanoparticles consisted of NETs. Transmission electron microscopy studies have shown that the rods were located in extracellular space (Figure 3C) and were not surrounded by membranes. Single extracellular fibres from the NETs could not be assessed directly but the ultrathin sections (Figure 3D) look comparable to reports in which 15 nm-sizing fibres were visualized.[7] Results were similar for monocytes and macrophages considering that in general fewer cells were involved into cell-particle networks, while dendritic cells and lymphocytes were not involved in the formation of extracellular traps.

None of the surface modifications of our particles were capable to prevent trapping by NETs. In contrast to this, uptake by macrophages is abolished by PEO-stabilization of nanoparticles even with the presence of charged functional groups at the nanoparticle surface.[8] Thus, extracellular trapping is a much more efficient mechanism of particle clearance that occurs temporally prior to endocytosis and that is largely independent of the surface chemistry. In-vivo mechanisms of pathogen clearance have to be independent of surface charge as pathogens, like our particles, can have any charge. They can be neutral, positively or negatively charged, or amphiphilic.[18] Bacteria and viruses are even capable of changing the charge of their surface to overcome the activities of antimicrobial peptides[18,19] that are part of the NET structures.[7] Nevertheless, the enhanced trapping of positive particles suggests that this mechanism is most efficient for similarly sized and positively charged viruses. For example, the positive surface charge of the herpes simplex virus UL42 mediates DNA binding of the pathogen.[20]

We show that not only neutrophils and mast cells form extracellular traps but that also monocytes and macrophages, which all belong to the myeloid lineage of immune cells, produce such structures. According to our results, B- and T-lymphocytes, the most important cell types of the lymphoid lineage, do not generate extracellular matrices (Figure 1). Consequently, we extend the definition of these extracellular fibres as extracellular traps of myeloid immune cells (ETMIC).

In this study, a novel clearance mechanism for nanoparticles by the human immune system has been described. We have demonstrated that extracellular traps are not only produced by neutrophil granulocytes but to a lower extent also by monocytes and macrophages. The amount of particles that is trapped strongly depends on the surface chemistry of the particles. However, also nanoparticles that are modified with PEO on the surface are trapped to a significant extent by these extracellular structures. Immune cell extracellular traps thus represent a putative barrier for nanoparticles and nanoparticle-based drug delivery systems and may contribute to nanoparticle clearance or even harmful solid aggregations of cells, particles, and extracellular structures when formed *in vivo*.

Acknowledgment. This work was supported by the DFG research training group "Biointerface" (GRK1035), the BMBF (13N9176 "Nano-SRT"), the EU (FP 6, IP NanoBioPharmaceutics) as well as the Interdisciplinary Centre for Clinical Research (IZKF "BioMAT") within the faculty of Medicine at the RWTH Aachen. TEM was performed at Electron Microscopic Facility (EMF), University Hospital, RWTH Aachen.

Supporting Information Available. Detailed description of the experimental procedures, gold nanorod and nanosphere coating, cell isolation, TEM control experiments for the seedless-deposition procedure, interaction studies with spherical particles and some additional experiments and discussion are available free of charge via the Internet at http://pubs.acs.org.

DOI: 10.1021/nl902830x | *Nano Lett.* **2010,** *10,* 59-63

REFERENCES AND NOTES

(1) Schwarzer, E.; De Matteis, F.; Giribaldi, G.; Ulliers, D.; Valente, E.; Arese, P. *Mol. Biochem. Parasitol.* **1999**, *100* (1), 61–72.
(2) Mollinedo, F.; Borregaard, N.; Boxer, L. A. *Immunol. Today* **1999**, *20* (12), 535–537.
(3) Auffray, C.; Sieweke, M. H.; Geissmann, F. *Annu. Rev. Immunol.* **2009**, *27*, 669–692.
(4) Cohen, M. S. *Clin. Infect. Dis.* **1994**, *18 Suppl 2*, S170–179.
(5) Brinkmann, V.; Reichard, U.; Goosmann, C.; Fauler, B.; Uhlemann, Y.; Weiss, D. S.; Weinrauch, Y.; Zychlinsky, A. *Science* **2004**, *303* (5663), 1532–1535.
(6) von Kockritz-Blickwede, M.; Goldmann, O.; Thulin, P.; Heinemann, K.; Norrby-Teglund, A.; Rohde, M.; Medina, E. *Blood* **2008**, *111* (6), 3070–3080.
(7) Gref, R.; Minamitake, Y.; Peracchia, M. T.; Trubetskoy, V.; Torchilin, V.; Langer, R. *Science* **1994**, *263*, 1600–1603.
(8) Bartneck, M. ; Keul, H. A.; Singh, S.; Czaja, K.; Bockstaller, M.; Möller, M.; Zwadlo-Klarwasser, G.; Groll, J. Submitted for publication.
(9) Pan, Y.; Neuss, S.; Leifert, A.; Fischler, M.; Wen, F.; Simon, U.; Schmid, G.; Brandau, W.; Jahnen-Dechent, W. *Small* **2007**, *3* (11), 1941–9.
(10) Keul, H. A.; Moeller, M.; Bockstaller, M. R. *J. Phys Chem C* **2008**, *112* (35), 13483–13487.
(11) Keul, H. A.; Moeller, M.; Bockstaller, M. R. *Langmuir* **2007**, *23* (20), 10307–10315.
(12) Jonuleit, H.; Kuhn, U.; Muller, G.; Steinbrink, K.; Paragnik, L.; Schmitt, E.; Knop, J.; Enk, A. H. *Eur. J. Immunol.* **1997**, *27* (12), 3135–3142.
(13) Jacobs, J. J.; Lehe, C. L.; Hasegawa, H.; Elliott, G. R.; Das, P. K. *Exp. Dermatol.* **2006**, *15* (6), 432–440.
(14) Kawamoto, H.; Minato, N. *Int. J. Biochem. Cell Biol.* **2004**, *36* (8), 1374–1379.
(15) Czarnetzki, B. M.; Figdor, C. G.; Kolde, G.; Vroom, T.; Aalberse, R.; de Vries, J. E. *Immunology* **1984**, *51* (3), 549–554.
(16) Ruhnke, M.; Ungefroren, H.; Nussler, A.; Martin, F.; Brulport, M.; Schormann, W.; Hengstler, J. G.; Klapper, W.; Ulrichs, K.; Hutchinson, J. A.; Soria, B.; Parwaresch, R. M.; Heeckt, P.; Kremer, B.; Fandrich, F. *Gastroenterology* **2005**, *128* (7), 1774–1786.
(17) van der Laan, L. J.; Ruuls, S. R.; Weber, K. S.; Lodder, I. J.; Dopp, E. A.; Dijkstra, C. D. *J. Neuroimmunol.* **1996**, *70*, 145–152.
(18) Nizet, V. *Curr. Issues Mol. Biol.* **2006**, *8* (1), 11–26.
(19) Brault, A. C.; Powers, A. M.; Holmes, E. C.; Woelk, C. H.; Weaver, S. C. *J. Virol.* **2002**, *76* (4), 1718–1730.
(20) Komazin-Meredith, G.; Santos, W. L.; Filman, D. J.; Hogle, J. M.; Verdine, G. L.; Coen, D. M. *J. Biol. Chem.* **2008**, *283* (10), 6154–6161.

DOI: 10.1021/nl902830x | *Nano Lett.* **2010,** *10,* 59-63